DETECTION RATE STATISTICS IN SYNTHETIC APERTURE SONAR IMAGES

Johannes Groen[a], Enrique Coiras[a], David Williams[a]

[a] NATO Undersea Research Centre, Viale San Bartolomeo 400, 19126 La Spezia, Italy.

Contact: J Groen, fax. +39 0187 527 331, groen@nurc.nato.int.

Abstract: *Synthetic aperture sonar (SAS) has proved to be successful for mine hunting and is now robust for generating high-resolution images over wide swath. The subsequent step in the processing is detection, discriminating between mine-like and non-mine-like objects, which is designed to minimise the number of missed mines so that the system can manage the detection rate. Statistical analysis using SAS has been limited, because operational use of the technology is at an early stage. The design of automated detection and classification systems depends however on these statistics, which for a SAS are environment dependent. NURC has collected a comprehensive data set off the coast of Latvia with the MUSCLE SAS, which comprises a wide range of seabeds, clutter and vehicle motion. The statistical analysis is based on 50 km^2 of SAS images at centimetre resolution.*

Keywords: *Synthetic aperture sonar, detection, mine hunting, statistics*

1. INTRODUCTION

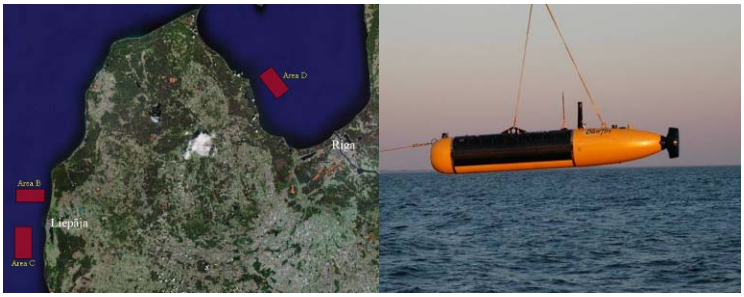

Fig.1: Colossus 2 trial off the coast of Latvia with predominant system MUSCLE.

Modern mine countermeasures (MCM) sonars have recently improved imaging resolution to such an extent that the traditional approach of post-processing is to be reassessed. The most successful methodology that has been achieving this resolution improvement is synthetic aperture sonar (SAS). The last decades this technology has been researched and is now well-understood in terms of requirements, robustness and sensitivity to environment and geometry. Operational use is limited however to a few countries.

This article focuses on a part of the signal processing chain that comes with SAS systems employed for MCM purposes. The signal processing chain roughly consists of imaging, followed by detection, classification and localisation. The part of interest in this article is the detection phase. In April 2008, NURC conducted a sequence of experiments off the coast of Latvia, which is illustrated in Fig.1 and resulted in a large dataset collected with the MUSCLE AUV equipped with a SAS operated around a frequency of 300kHz.

The outline of the article is as follows. Section 2 describes the dataset and its features. The detector is explained in Section 3, followed by the corresponding statistical analysis in Section 4. Section 5 discusses the impact on the MCM system and conclusions follow in Section 6.

2. DATASET OF SAS IMAGES

During the Colossus 2 trial mentioned in the previous section experimental data were gathered in order to support R&D on signal processing techniques and to establish the potential of AUVs with a high-resolution SAS. The signal processing techniques of interest are SAS imaging, automated detection and automatic target recognition. Owing to the excellent weather, the sea trial resulted in a total of 24 AUV missions in the areas B, C and D. The respective areas provided 12 (D), 21 (C) and 22 (B) km^2 of SAS images.

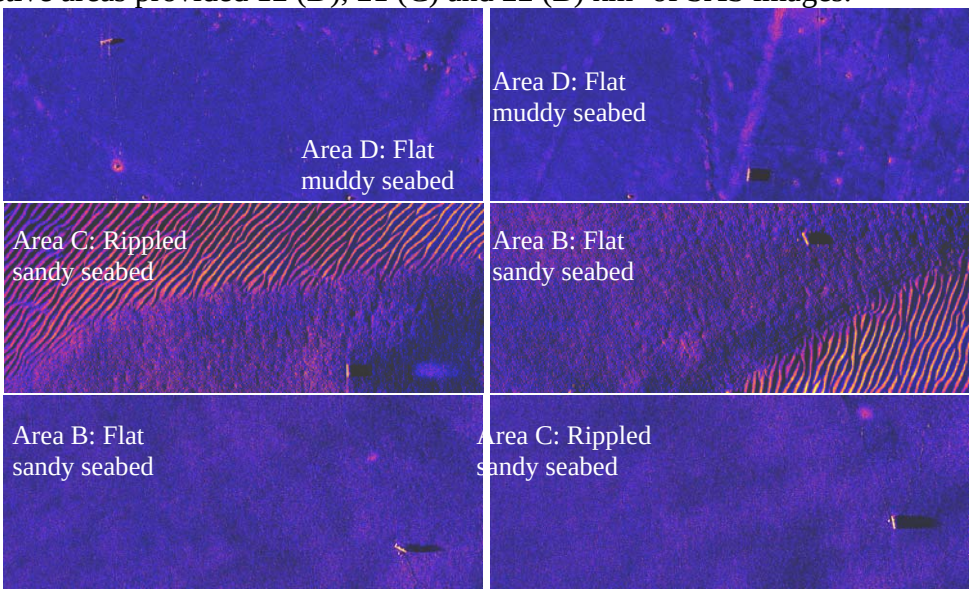

Fig.2: SAS images with a cylinder on different seabeds. Image dimensions are 40 m along-track and 100 m in slant range starting at 50 m and colour range is 40 dB.

Fig.2 gives an idea of the variety of images collected. From top to bottom the images are representative for area D, area C and area B, respectively. The images are normalised with a median filter so that range dependent echo strength due to the vertical beampattern and propagation loss is removed. In each area, AUV surveys were conducted and provided a

comprehensive MCM dataset that contains a large number of bottom types, false alarms (man-made and natural), and actual mines. In addition seven target shapes were deployed in each of the areas, and those were surveyed to obtain SAS images at different aspect angles and ranges. One target shape visible in the images in Fig.2 is an MP80 cylindrical mine shape. In area D often trawl marks were visible, and objects on the seabed are usually surrounded by a shadow and a patch of brightly scattering seabed, which indicates that the object is in a scour pit and has increased seabed roughness locally. Area C is a rather challenging area for MCM, especially when the targets are hidden within the ripples. In particular the detector phase is difficult when irregular ripples are present. Area B can be regarded most benign for MCM with SAS. The sonar signal correlation is always good, which results in constant good imaging performance. In addition to this, highlight and shadow are sharply defined on such seabed.

GPS positions of the targets were recorded during deployment and the targets were deployed far from other unknown objects for safety reasons. This enables ground truth on the targets: detection close to the recorded deployment can be concluded to be correct.

2.1. SAS issues affecting imaging and detection robustness

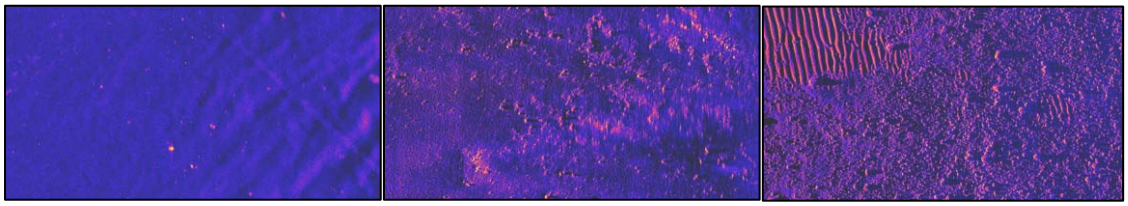

Fig.3: Three cases where detection of mines with a SAS is a challenge; from left to right: low scattering energy, sonar instability and high contact density. Dimensions are 50 by 100 m starting at 50m and colour range is 40 dB.

SAS performance degradation can have different causes, of which some were observed in this trial dataset. The most significant effect that all these causes have is an overall decrease in ping-to-ping correlation, leading primarily to difficulties in the sonar motion estimation and secondarily to integration of incoherent data. Both damage image quality. One of the causes is multi-path, especially second-order multi-path, which can have a rather destructive impact on the SAS image. In the dataset of this paper very few problems from multi-path were found owing to the relatively deep water of over 30 m and the narrow vertical beam design of the SAS. Another source that was observed was the influence of bottom type. In area D, consisting of mud, sometimes lack of signal occurred at long range, which causes low signal-to-noise ratio, in turn leading to low correlation, which can be seen in the left image of Fig.3. However, the most frequent effect in this dataset was sonar instability, which occurred at the beginning of a leg or when current was significant. When the vehicle is yawing within the SAS integration time some patches of sea floor are not insonified enough. Considering that the horizontal beamwidth is 6^o and that, at times, vehicle yaw variation was more than 3^o, it is no surprise that image quality then suffers. Nevertheless, it should be mentioned that none of these effects occurred very often and almost all images analysed were of good quality.

Regrettably, good SAS image quality is not the end of the story and no guarantee for target detection, which is also environment dependent. A part of area C with many pebbles and boulders is visible in the most right image of Fig.3. Even if the imaging characteristics are rather benign, the detector is facing many items that are typical for mines such as highlight and shadow.

3. DETECTOR

A detector of mines in SAS images aims to distinguish between mine-like objects and non mine-like objects. Since this is not the end station in the processing chain, the design of the detector can be regarded as merely a data reduction. For an automated system, the data reduction requirement is given by the next phase, the classifier. As long as the classifier, which may include better discriminative techniques [1], can handle the detector output, the system is well-designed. For this reason, it is important to keep the detector threshold low so that enough real mines pass. The detector itself should also be relatively simple, because it should not have a very strong discriminative behaviour (rocks of mine size are required to pass) and the detection algorithm has to be applied to the full dataset (22 Gigabyte per hour in this case). It is regarded as a first rough sifting of the data.

3.1. Approach and results

The core part of the detector analysed in this article is based on convolution with a template. Not much a priori knowledge or assumptions about the target are inserted at this stage. The template consists of a block of highlight (+1) and a block of shadow (-1) as described by [2]. The size of the template highlight area was set to 1m (along-track) by 0.5m (range). The width of the shadow was set to 0.5m and the (range-dependent) shadow length was computed with the altitude a and object height h. Before convolution with this template the SAS image is first normalised as described in [2]. After detection the scores also undergo a further normalisation step in order to make the statistical properties of the detection scores the same. When computing mean and variance of the detection scores, a range dependent trend appears. This trend is removed based on all the images, mean and variance are not range dependent after this step.

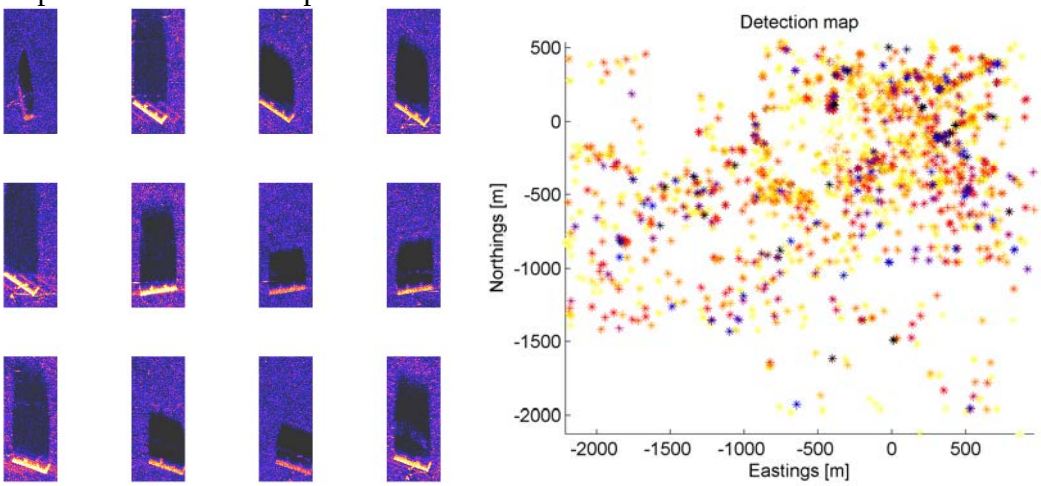

Fig.4: Detection results in area B with 12 detections (3 by 7 m) of the same cylindrical mine (left-hand side) and a detection map of the total area (right-hand side). Colour coding in the detection map is logarithmic with a dynamic range of 70 dB.

Fig.4 shows twelve detections around the position of the cylindrical mine. The image snippets of 3 by 7m are stored with location information and detection score. The detection map of area B after eight missions is shown in addition.

4. MEASURED DETECTION STATISTICS

The detector described in Section 3 was applied to the complete database of about 10^5 measured SAS images of dimensions 50 by 110 meters. The detection threshold was kept relatively low in order not to miss actual targets and to analyse higher thresholds as well. It is impossible to truly analyse false alarm rate in this dataset, because the ground-truth is incomplete. Detected objects can be false alarms, but can also be actual mine-like objects. However, since the target-deployment positions are known, we focus on the detection performance in terms of detection density ρ versus probability of missing a target P_{miss}. The dependence of these two parameters on bottom type and grazing angle is investigated.

The trial enabled detection assessment on bottom types different in nature as suggested by the top panel of Fig.5. These five types aptly covered the variability and are categorised as follows. Bottom type 1 is benign, flat and muddy, typically found in area B. Bottom type 2 consists of sand ripples, found in area C. Bottom type 3 is complex, with patches of sand ripples, pebbles & boulders, found in the northern part of area C. Bottom type 4 is benign, flat and sandy with little texture, found in area D. Bottom type 5 was found in areas C and D and is a mix of sand and small rocks/shells. The seabed was classified with unsupervised seabed segmentation, which resulted in bottom type estimate every 2 m^2 of SAS image as described in [4]. Here one estimate per SAS tile, the dominant one, is used.

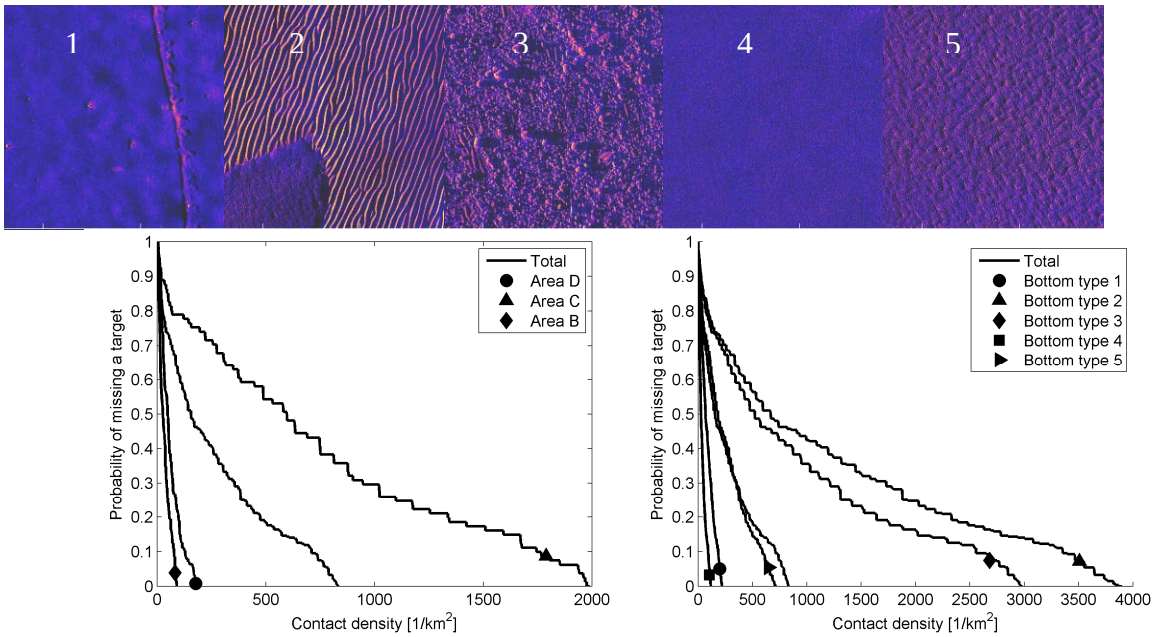

Fig.5: Typical examples of bottom types (top panel) and detection performance in the three trial areas (bottom left) and for the five different bottom types (bottom right). SAS image dimensions are 50 m by 50 m and logarithmic colour scale has a 40 dB range.

The left bottom plot of Fig.5 shows the performance of the detector described in Section 3. The probability P_{miss} is computed by varying the threshold τ and counting the number of targets with a detection score $\sigma(k)$ below the threshold

$$P_{miss} = \frac{\sum_{k \in \text{targets}} 1_{\sigma(k)<\tau}}{N_t} \qquad (1)$$

The total number of targets is given by N_t and k is the index for the detections. The contact density that corresponds to these values of P_{miss} and τ is computed with

$$\rho = \frac{\sum_k 1_{\sigma(k)>\tau}}{A} \tag{2}$$

The total area is denoted by A. The other three curves, for area D, C and B, are computed in the same way but using the subset of detections from each area, which is possible because the targets were deployed in each of the three areas. The results visible with these curves indeed show a rather strong dependence on area. The performance in area C is much worse, which is no surprise after interpreting the examples is Figs. 3, 4 and 5. Whilst contact density (for very low P_{miss}) is below 200 per km^2 in areas C and B, it is almost 10 times this value in area D.

The right bottom plot provides a better insight on the detection dependence on bottom type. Overall the areas B, C and D were different, but the bottom-type classes were found to give a more sensible subdivision. However, compared to the left-hand plot, P_{miss} had to be calculated differently, due to the fact that targets were only deployed on three out of five bottom types. No targets were deployed on bottom type 3 and 5. Instead all target detection scores were used for each of the curves and only the number of contacts corresponding to the bottom type was used. The right-hand side plot reveals an even stronger bottom type effect, with a low contact density (<200 per km^2) for bottom types 1 and 4 and a factor 30 to 40 worse for bottom types 2 and 3.

MCM detection and classification performance is known to depend on grazing angle γ. It is beneficial to image the target at shallow grazing angle so that it "sticks out". At steeper grazing angles highlight-to-reverberation ratio is lower and shadows are smaller. However, performance at shallower grazing angle (long range) is more sensitive due to the following five reasons: (1) SAS resolution gain is required to be higher to maintain constant resolution, (2) SAS becomes more sensitive to motion, (3) bathymetric variations cause increased shadow zones, (4) coherence and energy loss due to longer propagation, (5) multi-path.

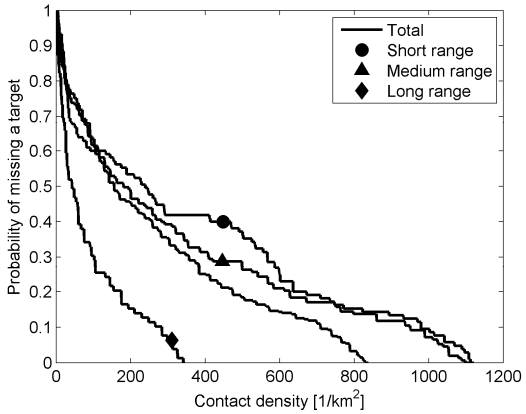

Fig.3: Detection performance versus range where short range is 40-70m, medium range is 70-110m and long range is 110-150m.

Fig. 3 shows that the suspected grazing angle dependence is indeed obvious in this data. During the trial the altitude of the vehicle was kept constant at a = 13 m, which enables to compute the grazing angles for these ranges r with $\sin\gamma = a/r$.

This means that the grazing angle values are 5-6.8^o for the long range set, 6.8-10.7^o for the medium range set and 10.7-19^o for the short range set. It is better to subdivide into grazing angle windows with equal width to highlight this dependence, but unfortunately here this led to insufficient statistical information in the short range set.

5. IMPACT ON MINE HUNTING AUV SYSTEM

The results presented in the previous section prove the strong influence of bottom type and geometry (grazing angle) on detection statistics and performance. The performance was analysed in terms of contact density, which is an important parameter in further analysis. The contact density can be related to contact frequency f (contacts per hour) and to detector's data reduction factor d. The contact frequency is $f = 2\rho v(r_{\max} - r_{\min})$.

The velocity of the AUV is given by v = 1.5 m/s, the maximum range $r_{\max}$ = 150m and the minimum range $r_{\min}$ = 40m. The data reduction factor d is given by

$$d = \frac{1}{\rho l w} \tag{3}$$

In this analysis the dimensions of the snippet are set to l = 7m and w = 3m, in range and along-track, respectively. Contact frequency f is an essential parameter when human operators are involved in the classification process; it reveals how much information the operator has to analyse. For computer automated classification the essential requirement is data flow. The classification algorithms are usually sophisticated and computationally expensive, and cannot be applied to the complete data set. The parameters for the different bottom types can be found in Table 1.

Bottom type	ρ [1/km^2]	f [1/hour]	d
1	200	238	238
2	3800	4514	13
3	2900	3445	16
4	100	119	476
5	600	713	79

Table 1: Detection performance for the considered bottom types in terms of contact density ρ, contact frequency f and data reduction factor d.

From Table 1 it can be concluded that the output data flow varies from 90 Megabytes/hour in the easiest case to 1.75 Gigabytes/hour in the hardest case. It has yet to be verified how much this can be enhanced with an improved detection scheme, which is for instance tuned to discard typical false alarms such as fish and ripples. On the other hand, the requirement for the detector needs to be established. Intuitively, it would seem that a data reduction of around 20 is not sufficient, but it may well be that the automatic classifier can cope with such a dataflow. Visual analysis on the detection snippets does suggest that there is a quick gain expected when further improving the detection algorithm. The detector can easily be tuned to discard typical false alarms such as fish and ripples.

6. CONCLUSION

In this paper detection of mines in SAS images is investigated. In April 2008 NURC collected a comprehensive dataset with variations in bottom type, target type and geometry. This dataset proved useful for analysis of a detector in a statistical manner. The detection algorithm was applied to 10^5 SAS images, and after thresholding with a very low threshold resulted in a total number of detections of 60,000. The relationship between detected contacts and missed targets was established for the dataset and for subsets of certain bottom type. In addition, a similar analysis was performed to reveal the influence of grazing angle. Both bottom type and grazing angle showed to be important for the detector. These results were shown to have an importance for the design of an automated MCM detection and classification system.

7. ACKNOWLEDGEMENTS

The authors would like to thank Dr. Benjamin Evans, scientist in charge of the Colossus2 trial.

REFERENCES

[1] **S. Reed, Y. Petillot & J. Bell**, An Automatic Approach to the Detection and Extraction of Mine Features in Sidescan Sonar, *IEEE Journal of Oceanic Engineering*, Vol. 28, No. 1, (2003).

[2] **J.A. Fawcett & V. Myers**, Computed-aided classification for a database of images of minelike objects, Tech. Mem. TM 2004-272, Defence R&D Canada-Atlantic, Halifax, Canada, March 2005.

[3] **E. Coiras, J. Groen, D.P. Williams, B. Evans & M.A. Pinto**, Automatic change detection for the monitoring of cluttered underwater areas, In *Proceedings of the first international conference on Waterside Security*, Copenhagen, Denmark, August 2008.

[4] **D.P. Williams**, Bayesian Data Fusion of Multi-View Synthetic Aperture Sonar Imagery for Seabed Classification, *IEEE Transactions on Image Processing*, Accepted for publication February 2009.